Chapter 1

FEM Analysis of Mechanical and Structural Properties of Long Fiber-Reinforced Composites

Michal Petrů and Ondřej Novák

Additional information is available at the end of the chapter

http://dx.doi.org/10.5772/intechopen.71881

Abstract

This chapter deals with studies of the mechanical properties of samples from long fiber-reinforced composite structures that would contribute to the optimization of the developed constructions made of them. First, the basic issues of composite structures reinforced with long fibers (carbon or glass) and generally of composites with the specification of parameters that would lead to the optimization of mechanical properties with respect to the theoretical strength are presented. Further, the possibilities and methods of measurements of composite reinforced with carbon and glass fibers are described. This is followed by the introduction of analytical models for the description of the transversal isotropic composite, where these mathematical relations allow the determination of unknown elastic constants and they are also important for the verification of numerical models. Finally, it is comprehensively outlined the problems of creating a numerical model of advanced composite fibrous structure for determining the mechanical properties, both through the description of the continuum, and complex numerical model with a structural configuration enabling approach to allow closer interaction among fibers and matrix. Compared to the averaged values obtained from experimental samples, numerical simulations show a similar trend of stress on strain, with results obtained from simulations.

Keywords: FEM, composite structures, testing, mechanical properties, nonlinear properties

1. Introduction

Studies and analyses of mechanical properties of long fiber-reinforced composites provide important information for future lightweight constructions. First of all, it is important to approach the issues and specifics of long fiber-reinforced composite structures to increase the strength and toughness of the resulting structure. The long fiber-reinforced composite structure is typically formed from two dominant components: carrier fiber reinforcement and a

matrix. Ideal arrangement of the final composite (fiber-matrix connection), due to synergy, the high specific properties (high strength, stiffness, and toughness) can be achieved, where none of input components reached. It is that the optimal synergistic effect is characterized by a known "illogical" rule 2 + 3 = 7, which characterizes the sum of the properties of the individual input components (fibers + matrix) achieves a higher value of the specific properties of the newly created structure. In general, the highest specific properties can be achieved if the fibers are stressed up to the strength limit $\sigma_M^f\Big|_{F^f \to \max}$ with stress transferred with matrix. The matrix transforms the stress into the fibers, and it also has a significant effect on the bonding with the fibers. Thus, the matrix is the binder component of the composite, creating the final geometry of the composite and at the same time protecting the fibers from wear and damage, which would lead to loss of stability and strength of the resulting composite. The description of the properties of composite structures reinforced with long fibers due to their potential and specific characteristics was given by the authors namely Agarwal et al. [1], Guedes [2], Gay and Gambelin [3], Reifsnider [4], Teply and Reddy [5], Berthelot [6], Gibson [7], or Soden et al. [8]. The authors agree that long fiber-reinforced composite structures are unique materials whose mechanical properties cannot be generally described in an analytical or experimental manner. Theories also differ in mathematical relationships derived for unidirectional composite structures, let alone complete synthesis of mechanical properties for geometrically complex structures of frames with multidirectional fibrous arrangement. This is due to the fact that their properties vary significantly with the type of fibers and a matrix (e.g., physical and mechanical properties, surface treatment, chemical compositions, binding agents, density, thermal expansion, etc.) because only a slight change forms various combinations with significantly different properties in mechanical behavior.[1] Generally, long fiber-reinforced composite structures can be considered as inhomogeneous and heterogeneous structures with anisotropic properties in terms of physical and mechanical behavior. Their heterogeneity is manifested by a large number of combinations of different variants of the resulting structural materials suitable or unsuitable for the specific design requirements and load.[2] If the strength of the composite has to be maximized, the specific surface of the fiber-matrix interface must be high and free of defects. The selection of fiber reinforcement is possible to use a wide range of fibers, whereas their offer is developed and expanded. For structural applications such as frames for machine parts and equipment may be used virtually any organic natural fibers (e.g., coconut, cotton, cellulose fibers, etc.) from a variety of polycrystalline ceramic materials, polymeric fibers, glass, or carbon fibers. The production technology of these fibers is well described by Bareš [9]. Carbon fibers are industrially manufactured with a diameter of 5–12 μm by various methods such as carbonization of organic fibers or pyrolysis. It is generally known that carbon can exist in nature in three forms: diamond, graphite, and glassy (amorphous). Carbon fibers can be

[1] This can be mentioned in the example given by Bareš [9]. A simple combination of three homogeneous isotropic light metals to form ternary cast iron is obtained 82,160 possible variants of alloys, if more six metals are combined, more than 300 million different alloy variants could be obtained. (The composite structure reinforced with long fibers has a similar behavior, where the change of the matrix, directional arrangement, and type of fiber significantly affect resulting mechanical properties because it leads to qualitatively different structure [10]).

[2] Transmission of static stress applied to the composite and transferred with fibers is required excellent consistency of fibers and matrix; on the contrary, a dynamic impact requires energy absorption by the crack propagation along fibers.

considered as fibers produced at 800–1600°C, and graphite fibers are produced at >2200°C. However, only fibers obtained from the crystalline form of carbon arranged in a certain direction (production under tension) have a high elastic modulus and other specific design parameters such as a lower density, higher surface area, lower thermal conductivity, higher electrical resistance, and so forth compared to graphite fibers. Glass fibers with diameter of 3.5–20 μm are produced by fast drawing from the melts (the speed reaches up to 400 m min^{-1}). The spinning speed is also influenced by the viscosity (50–100 Pa s), the melting temperature,

Figure 1. Example: Low strength of the fiber composite structure due to the poor joint of the fiber with matrix.

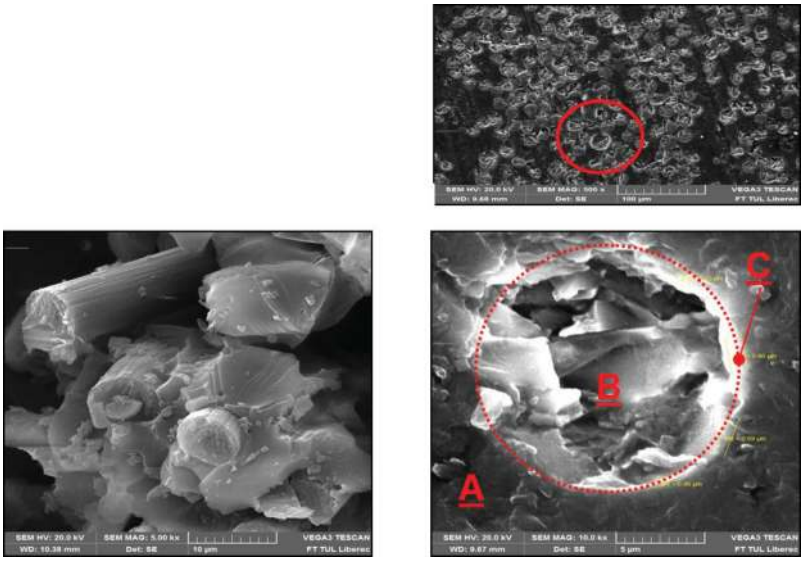

Figure 2. Cross section of composite sample with long fibers (upper), detail: fiber-matrix (bottom left), detail: phase interface (bottom right).

and, of course, the chemical composition of the glass. The matrix, which affects the properties and usability of the resulting composite, has been epoxy used for both the testing sample and design of the developed composite construction. The composite production may result in imperfect bonding of the matrix fibers (e.g., low wettability of the fiber reinforcement in the matrix, bubble formation, etc.), which leads in mechanical defects in the composite structure, which often over grow into critical defects with a significant reduction in strength (**Figure 1**). The resulting strength of the composite structure affects mechanical properties of the selected fiber reinforcement and matrix, which are characterized by mechanical parameters, for example, the elastic modulus, Poisson number, or other parameters such as the creep and fracture properties of the individual components. In terms of strength, a significant role (if not most) plays the interfaces among the fibers and the matrix, which is shown in **Figure 2**. This is due to the fact that the characteristic properties of the interface create a mechanism that apparently causes the synergistic effect that provides their unique mechanical properties to composite structures. Although a number of theories have been compiled, the synergistic mechanism of the phase interface is not yet clear.

2. Measurement of mechanical properties of composite samples with long fiber reinforcing

The determination of unknown parameters of composite materials has to be performed by experimental measurements. These parameters represent input data for numerical simulations. For a complete description of the properties, it is important to make measurements on both the fiber reinforcement (tow) and the matrix as well as on the resulting long fiber-reinforced composite structures (matrix-bonded fibers). Measurement of the mechanical properties of the samples is carried out according to standard laboratory tests, which are divided according to the time course of the applied load. Tests can be divided into static and dynamic. It can thus perform the tensile test at a constant or cyclic loading of the sample, three-point bending strength, and Charpy impact test, as shown in **Figure 3**. The samples may be formed in the "dog bone" shape or, optionally, in the form of a rectangle of defined length L, width b, and thickness h,[3] whereas they can be used for short- or long-term test.

The characteristic physical properties of samples of long fiber-reinforced composites are influenced by weight and volume ratios of individual input components (fiber reinforcement and matrices) that ultimately affect design parameters (mechanical properties and weight of the structure). The mass and volume amounts of the fibers and the matrix in the composite structure sample can be defined according to the following relationships (1–5).

$$m^c = m^f + m^m \tag{1}$$

$$M^f = \frac{m^f}{m^c}, \quad M^m = \frac{m^m}{m^c} \tag{2}$$

[3]Note: geometrical dimensions h, b, L can be also smaller, but it can lead to a problem with clamping of the sample to the jaws of dynamometer.

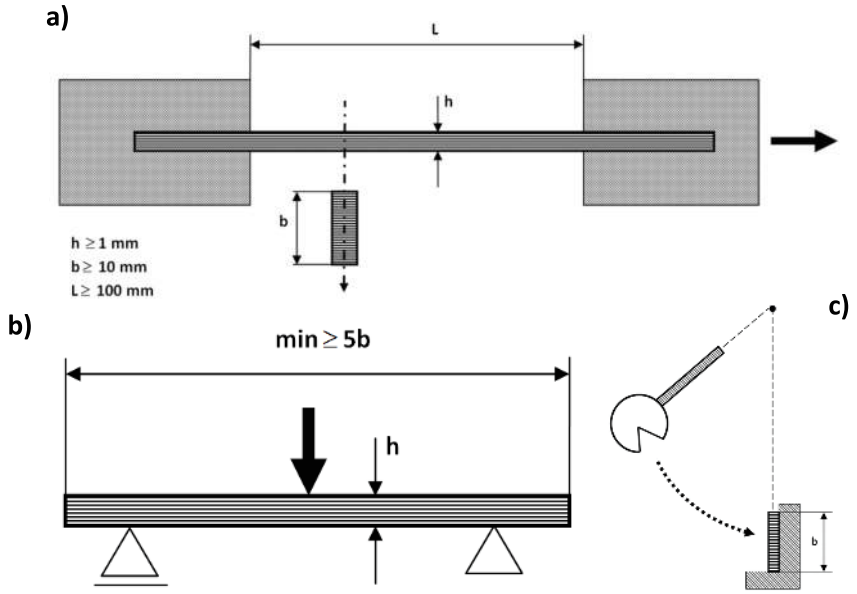

Figure 3. Determination of mechanical properties of composite samples: (a) tensile test, (b) three-point bending test, and (c) Charpy impact test.

$$M^f = 1 - M^m \tag{3}$$

$$V^f = \frac{\mathrm{v}^f}{\mathrm{v}^c}, \quad V^m = \frac{\mathrm{v}^m}{\mathrm{v}^c} \tag{4}$$

$$V^f = 1 - V^m \tag{5}$$

where m^c is the total weight of composite, m^f, m^m is the weight of fibers and matrix, M^f, M^m is the weight amount of fibers and matrix, V^f, V^m is the volume amount of fibers and matrix, v^c is the total volume of composite, and $\mathrm{v}^f, \mathrm{v}^m$ is the volume of fibers and matrix. Volume amount of fibers V^f and matrix V^m can be also expressed with the help of the fiber density ρ^f and matrix density ρ^m, which is applied in Eq. (6). The total density $\rho^c = m^c/\mathrm{v}^c$ can then be expressed as the sum of components, that is, the reinforcement and matrix (7). The characteristic thickness of the composite structure can be expressed according to the relationship (8).

$$V^f = \frac{M^f/\rho^f}{M^f/\rho^f + M^m/\rho^m}, \quad M^f = \frac{V^f\rho^f}{V^f\rho^f + V^m\rho^m} \tag{6}$$

$$\rho^c = \rho^f V^f + \rho^m V^m \tag{7}$$

$$h = m^f\left[\frac{1}{\rho^f} + \frac{1}{\rho^m}\cdot\left(\frac{1 - M^f}{M^f}\right)\right] \tag{8}$$

Gay and Hoa [10] reported that winding of the fibers onto-shaped geometry may achieve the

Name of fibers	m^{f*} [g m^{-2}]	m^{m*} [g m^{-2}]	M^f [%]	M^V [%]	V^f [%]	V^m [%]	ρ^f [g cm^{-3}]	ρ^m [g cm^{-3}]	h [mm]
GF 1600 tex/PUR Huntsman	560	600	48	52	30	70	2.45	1.1	1.2
CF prepreg HEXPLY-M10R	150	91.96	62	38	52	48	1.8	1.2	0.22
CF 24K/PUR Huntsman	213	747	22	78	15	85	1.8	1.1	1.2

Note: m^{f*}, m^{m*} represent area weight, m^{c*} is the total weight of composite.

Table 1. Examples of physical and geometrical parameters of the selected samples of composite structures reinforced with long fibers.

volume fraction of fibers in the composite maximally 55–80% of the total volume of the composite structure. Ideally, these values can be increased by precisely placing fiber tows side by side. A limit state of volume fiber fraction, that is, 100%, cannot be achieved due to the necessity of the presence of the matrix. Also by perfectly precise laying of fiber strands, the strands will always have a certain fill value that will never be equal to 1 in the geometric configuration. Perfectly precise laying of fiber tows does not provide 100% of volume filling due to fiber cross section. However, it should be noted that the optimum ratio of fiber reinforcement is in the range of the synergistic effect, that is, $V^f \approx 0.4 \div 0.65$.

The influence of selected physical parameters on the geometric parameter h of some tested samples from long fiber-reinforced composite structures is shown in **Table 1**. These parameters can then be used to establish numerical models. Other input parameters that are required for the numerical model have to be obtained by measuring the test samples. Other input parameters that are necessary for the numerical model are obtained by testing composite samples.

3. Analytical models for the study of mechanical properties of long fiber-reinforced composites

Numerical modeling of the mechanical properties of the composite is a very difficult problem because there are many unknown parameters that come into model simulations, which are discussed in this chapter. Therefore, some parameters need to be properly verified with analytical models. It is assumed that though mechanical properties of the sample are formed from uniformly spaced transversely isotropic structure, its theoretical description is difficult, as shown in **Figure 4**.

The model of the transverse isotropic fiber composite structure can be defined by six independent elastic constants through the constitutive Eq. (9). The mechanical properties, such as composite structures, are also affected by the volume of fibers V^f and matrix V^m.

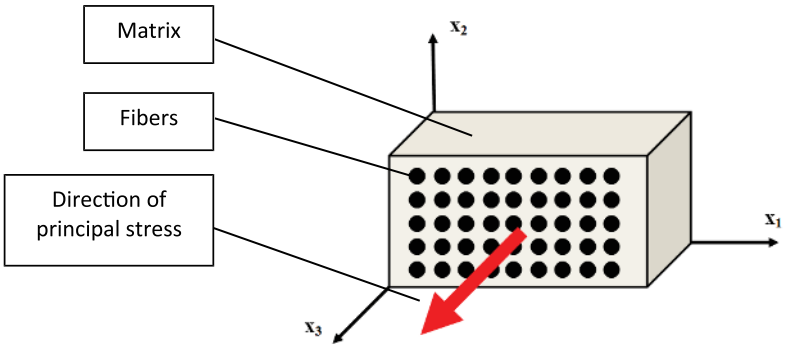

Figure 4. Model of idealized transverse isotropic fiber composite structure.

$$\begin{Bmatrix} \varepsilon_{11} \\ \varepsilon_{22} \\ \varepsilon_{33} \\ \gamma_{12} \\ \gamma_{23} \\ \gamma_{13} \end{Bmatrix} = \begin{bmatrix} 1/E_{11} & -\nu_{12}/E_{11} & -\nu_{12}/E_{11} & 0 & 0 & 0 \\ -\nu_{12}/E_{11} & 1/E_{22} & -\nu_{23}/E_{22} & 0 & 0 & 0 \\ -\nu_{12}/E_{11} & -\nu_{23}/E_{22} & 1/E_{22} & 0 & 0 & 0 \\ 0 & 0 & 0 & 1/G_{23} & 0 & 0 \\ 0 & 0 & 0 & 0 & 1/G_{12} & 0 \\ 0 & 0 & 0 & 0 & 0 & 1/G_{12} \end{bmatrix} \cdot \begin{Bmatrix} \sigma_{11} \\ \sigma_{22} \\ \sigma_{33} \\ \tau_{12} \\ \tau_{23} \\ \tau_{13} \end{Bmatrix} \tag{9}$$

where $\sigma_{ii}, \varepsilon_{ii}$ are the principal stresses and strains in the transversal isotropic composite in individual directions of the coordinate system x_1, x_2, x_3, whereas $\sigma_{11} > \sigma_{22} = \sigma_{33}$, $\varepsilon_{11} \neq \varepsilon_{22} = \varepsilon_{33}$, and $\tau_{12}, \tau_{23} = \tau_{13}$ are the shear stresses in the given planes, $\gamma_{12}, \gamma_{23} = \gamma_{13}$ expresses the shear to individual planes, $E_{11}, E_{22} = E_{33}$ expresses the longitudinal and transverse modulus of elasticity, G_{12}, G_{23} is the shear modulus in the plane of the principal load direction and in a plane perpendicular to the principal load direction, ν_{12} is the Poisson ratio in the principal direction of the load, and ν_{23} is the Poisson ratio in a plane perpendicular to the principal load direction.

For the corresponding model, the interconnection of individual components A, B, C must be included (see **Figure 2**) to create a multiphase system approaching the behavior of composite structures. Therefore, the problem of modeling a composite can be treated as a continuum (a solid model without a geometric arrangement of individual components) or by creating a completely new model with structural parameters, that is, the individual components will be included in the structured unit. The problem of analytical modeling of mechanical properties of general fiber structures through a structural unit is described, among others, by Wyk for the study of interfiber contacts [11] and by Neckář [12]. However, the description of the mechanical properties of the fibrous composite structure is more difficult and has not yet been properly described. This is probably due to the fact that knowledge of the deformation mechanism and damage process is more important for understanding the mechanical properties than the knowledge of the absolute strength that cannot be determined with sufficient precision. This is due to the fact that it is not possible to comprehensively construct a general energy theory (to derive empirical relationships for deformation work) based on statistical

characteristics, as can be done with very good accuracy for other anisotropic structures (Petrů et al. [13, 14]). The problem is that the individual components composing the composite structure cannot be reliably quantified even with homogeneous isotropic materials (matrices, glass fibers), let alone anisotropic structures such as carbon fibers (the theoretical value presented in the data sheet is different than value determined experimentally). Therefore, the main problems are related to the complexity of the description and modeling of deformation and the consequent character of the stress (stress concentration under loading). This is mainly due to technological influences in composite production (influence of temperature, humidity, and initial microporosity) that cannot be predicted for model simulations, and it is also relatively difficult to experimentally identify these parameters.[4]

Over time, there have been widespread analytical relationships to form the approach to obtain all elastic constants that can be used by these models, which are given as follows:

- phenomenological models.
- semiempirical models.
- homogenized models.

3.1. Phenomenological models

In the past, phenomenological models have been created as the primary mathematical derivation of the mechanical properties of transversally isotropic fibrous composite structures but can be used well today. Such models include the Voigt and Reuss models. These are models using the mixing rule (mixing of the individual input components, i.e., fibers and matrices), while the Voigt model is very well usable for determining the elastic constants E_{11},ν_{12} defined by relationships (10 and 11) and is characterized by isotropic strain. The Reuss model is usable for determination E_{22}, G_{12} defined by relationships (12 and 13) and unlike the Voigt model is characterized by isotropic stress.

$$\frac{d\sigma_{11}}{d\varepsilon_{11}} = V^f \frac{d\sigma^f}{d\varepsilon^f} + V^m \frac{d\sigma^m}{d\varepsilon^m} \;\Rightarrow\; E_{11} = V^f E_{11}^f + V^m E^m \tag{10}$$

$$\nu_{12} = V^f \nu_{12}^f + V^m \nu^m \tag{11}$$

$$E_{22} = \frac{E_{22}^f E^m}{E^m V^f + E_{22}^f E^m} \tag{12}$$

$$G_{12} = \frac{G_{12}^f G^m}{G^m V^f + G_{12}^f E^m} \tag{13}$$

[4] In the advanced model, simulations can be assembled material models with any parameters, including the statistical parameters, which describe technological production factors, for example, through the theory of random fields as defined by Bittnar and Šejnoha [15]. The problem lies in the identification of the effects and the subsequent statistical evaluation.

where E_{11}^f, E_{22}^f are the longitudinal and transverse modulus of the fiber elasticity, G_{12}^f is a fiber shear module, and ν_{12f} is the Poisson ratio in the plane of the principal direction of the load of the fiber.

3.2. Semiempirical models

Semiempirical models were created later than phenomenological models, and based on the new information and knowledge, they are still being updated. Their development led in particular to the further expansion of the Voigt and Reuss models because these models have been modified by correction factors to specify the resulting elastic constants for the given types of input components. This category includes models that are implemented in certain modifications in finite element softwares such as the Halpin-Tsai model or the Chamis model.

- **Modified model according to the mixing rule**

Modified model according to the mixing rule is derived from Voigt [16] and Reuss [17], and for elastic constants, E_{11}, ν_{12} is defined according to Eqs. (10 and 11). Modification occurs with constants E_{22}, G_{12}, because the resulting difference between the results obtained by the measurements and the relationships (12–13) is usually noticeable. Therefore, it was necessary to make a correction for E_{22}, G_{12} according to Eqs. (14 and 15).

$$\frac{1}{E_{22}} = \frac{\zeta^f V^f}{E_{22}^f} + \frac{\zeta^m V^m}{E^m} \tag{14}$$

$$\frac{1}{G_{12}} = \frac{\frac{V^f}{G_{12}^f} + \frac{\zeta' V^m}{G^m}}{V^f + \zeta' V^m} \tag{15}$$

where ζ^f, ζ^m are correction factors,[5] according to Younes et al. [18].

- Halpin-Tsai model

This is a model that is implemented in a number of numerical programs by using finite element method (FEM). This model is developed as a semiempirical model [19] with correction of E_{22}, G_{12}. Its semiempirical derivation (16–17) using correction factors ζ, ξ has a very good agreement with experiments.

$$E_{22} = E^m \left(\frac{1 + \xi\zeta V^f}{1 - \zeta V^f} \right) \tag{16}$$

$$G_{12} = G^m \left(\frac{1 + \xi\zeta V^f}{1 - \zeta V^f} \right) \tag{17}$$

[5]Correction factors ζ^f, ζ^m can be express as $\zeta^f = \frac{E_{11}^f V^f + \left[\left(1 - \nu_{12}^f \nu_{21}^f\right) E^m + \nu^m \nu_{21}^f E_{11}^f\right] V^m}{E_{11}^f V^f + E^m V^m}$, $\zeta^m = \frac{E^m V^m + \left[\left(1 - \nu^m \nu^m\right) E_{11}^f - \left(1 - \nu^m \nu_{12}^f\right) E^m\right] V^f}{E_{11}^f V^f + E^m V^m}$, ζ' is a variable function $0 < \zeta' < 1$, whereas preferred is $\zeta' \approx 0.5 - 0.6$.

where ζ correction factor, for which it is valid $\zeta = \frac{M^f/M^m - 1}{M^f/M^m + \xi}$, ξ is constant, which is for E_{22} equal to 1, and for G_{12} is equal to 2, $M = E$ or G in the case of an expression E_{22} and G_{12} according to Eqs. (12–13).

- Chamis model

This is another semiempirical model [20], which was unlike previous models developed not only for independent elastic constants $E_{11}, E_{22}, G_{12}, \nu_{12}$ but also for G_{23}. The determination of E_{11}, ν_{12} is again based on Voigt and Reusse according to Eqs. (10–11). The Chamis model for calculating other elastic constants introduces a square root of the volume of fiber $\sqrt{V^f}$, which has in Eqs. (18–20), the meaning of fiber incompressibility, which is in line with principle of mass conservation.

$$E_{22} = \frac{E^m}{1 - \sqrt{V^f}\left(1 - E^m/E_{22}^f\right)} \tag{18}$$

$$G_{12} = \frac{G^m}{1 - \sqrt{V^f}\left(1 - G^m/G_{12}^f\right)} \tag{19}$$

$$G_{23} = \frac{G^m}{1 - \sqrt{V^f}\left(1 - G^m/G_{23}^f\right)} \tag{20}$$

where G_{23}^f is the shear modulus of the fiber elasticity in a plane perpendicular to the principle direction of loading.

3.3. Homogenized models

Homogenized models are generalized models that can be used to determine very accurate values of elastic constants for developed composite structures reinforced by longitudinally laid fibers. Such models include, for example, the Mori-Tanaka model [21], a consistent model created by Hill [22] or the Bridging model. Their applicability compared to phenomenological or semiempirical models largely limits the more difficult determination of all constants entering to homogenized models. An example is the Eshelby toughness tensor that can be used for inclusion, which is introduced in both the Mori-Tanaka model and the consistent model. In view of this, from homogenized models, the Brindling model can be used to determine the elastic constants.

- Bridging model

This is a model that is developed to predict the stiffness and strength of transverse isotropic fiber composites. The elastic properties are for the elastic modulus E_{11}, ν_{12} the same as for Voigt and Reusse models (10–11). Elastic constants E_{22}, G_{12}, G_{23} can be expressed using the Bridging model (21–23).

$$E_{22} = \frac{\left(V^f + V^m a_{11}\right) \cdot \left(V^f + V^m a_{22}\right)}{\left(V^f + V^m a_{11}\right)\left(V^f S_{11}^f + V^m a_{22} S_{22}^m\right) + V^f V^m \left(S_{21}^m - S_{21}^f\right) a_{12}} \tag{21}$$

$$G_{12} = \frac{\left(V^f + V^m a_{66}\right) \cdot G_{12}^f G^m}{V^f G^m + V^m a_{66} G_{12}^f} \tag{22}$$

$$G_{23} = \frac{1/2\left(V^f + V^m a_{44}\right)}{V^f\left(S_{22}^f - S_{23}^f\right) + V^m a_{44}\left(S_{22}^m - S_{23}^m\right)} \tag{23}$$

where a_{ii}, $S_{ii}^{f,m}$ are the matrix components, which relate to fiber and matrix ratios in the composite structure as reported by Huang [23, 24], where $a_{11} = E^m/E_{22}^f$, $a_{22} = a_{44} = 0,35 + (1 - 0,35)\, E^m/E_{22}^f$, $a_{66} = 0,3 + (1 - 0,3)\left[0,5E^m/(1 + \nu^m)\right]/G_{12}^f$, $a_{12} = \left(S_{12}^f - S_{12}^m\right)(a_{11} - a_{22})/\left(S_{11}^f - S_{11}^m\right)$, $S_{11}^{f,m} = 1/E_{11}^{f,m}$, $S_{22}^{f,m} = 1/E_{22}^{f,m} S_{12}^{f,m} = S_{21}^{f,m} = -\nu_{12}^{f,m}/E_{11}^{f,m}$, $S_{23}^{f,m} = S_{32}^{f,m} = -\nu_{23}^{f,m}/E_{22}^{f,m}$.

4. Numerical models for the study of mechanical properties of long fiber-reinforced composites

Measurement and analytical models of long fiber-reinforced composite structures designed to study mechanical properties are generally able to provide only limited information. This is due to the fact that the measurements are limited by the possibilities of positioning of the sensors and also by the fact that some properties cannot be measured well (e.g., the distribution of the main stress and deformation in the composite structure). The knowledge of the distribution of the main stresses and deformations in the structure is important for assessing how the structure is changed and under which stress. In this case, the corresponding model simulation using numeric methods represents a significant support for the development. Very suitable is to build model simulation in finite element method (FEM), but other numerical methods, such as discrete element (DEM), boundary element (BEM) or finite volume method (FVM) method, are also available. The mechanical loading of composite causes many different processes in the inner structure that varies with the actual deformation. Therefore, it is necessary to simplify or neglect some characteristic features in modeling of such structures. A major problem of mechanical properties modeling of composite structures is in particular the description of the principal stresses in short time $\Delta t = t_{i+1} - t_i$. The solution of problem of composite with boundary conditions under tensile loading lies not only in the specification of the correct boundary conditions and material properties but also in the design of the proposed finite element mesh. The FEM programs are currently very sophisticated and allow the solution of a continuous problem transform into a final solution where the corresponding geometric simple subareas (finite elements) can be designed in the preprocessor. Let $\Omega \subset \Re^3$ is the continuous area of the three-dimensional space in which the problem is solved. Its borders

will be denoted Γ, where Γis Lipschitz border and let the approximation of the selected base functions is derived above each finite element of length $l_{element}$, because any continuous function can be represented by a linear combination of algebraic polynomials converging to a continuous solution, that is, $\lim_{l_{element}\to 0} \to 1$. Thus, the FEM method can be understood as a special type of variation method by using the mathematical description of the problem solution. The current commercial software and FEM programs (e.g., Ansys, Abaqus, Permas, LS-Dyna, Marc, PAM CRASH) allow to assemble and subsequently solve a series of problems with nonlinear materials not only with elastic but also plastic behavior corresponding to the properties of the long fiber-reinforced composite.

4.1. FEM simulation of mechanical properties of long fiber-reinforced composite

Model simulations in FEM were performed for different combinations of reinforcement arrangements of long fiber-reinforced composites, which are important for comparison with experiments and analytical relationships. This gives the material properties for numerical simulation of the strength characteristics of whole frames.

This chapter describes the creation of two numerical models and their comparison:

(I) continuum model

(II) extended continuous model with structural unit

The simulations were performed for a complete assessment of the mechanical properties $\sigma_{11}, \sigma_{22}, \varepsilon_{11}, \varepsilon_{22}, \gamma_{12}, \gamma_{23}$ and elastic constants $E_{11}, E_{22}, G_{12}, G_{23}, \nu_{12}, \nu_{23}$, whereas also information explaining the shape changes of the samples observed especially during tensile stress. Model simulations were performed in the following steps:

- creating two model simulations of the long fiber-reinforced composite,
- creating the corresponding mesh of finite elements of the computational model in the preprocessor,
- defining the corresponding initial and boundary conditions,
- assembling a material model of the long fiber-reinforced composite,
- the evaluation and comparison of model simulation results in postprocessor.

4.1.1. Assembling of continuum of the long fiber-reinforced composite model

The FEM model was created in the concept of coherent continuum consisting of a surface geometry corresponding to the test sample with length L = 100 mm, width b = 20 mm, and thickness h = 1.7 mm. The finite element mesh of the numerical model was created from SHELL elements (2D elements) with a constant element size of 2 mm. The boundary conditions affecting the magnitude of the displacements and stress can be defined in two ways, that is, the boundary conditions of the first and second types. The first way is to determine the displacement and stress distributions if force conditions are known, that is, volume forces, surface forces, and nodal loads. The other way is to determine the displacement and tension distribution if the geometric conditions are known, that is, the size of node displacement, the

deformations, and so on. Both ways can be also combined. It is mixed boundary conditions, as shown by Li [25]. Boundary and initial conditions for the model were made by the boundary conditions of the second type. One side of the sample was fixed against the displacement and rotation of nodes $U_i = R_i = 0$ in all directions (layout), and the opposite side of the edge of the sample was fixed identically; only in X direction, the movement was allowed, whereas $U_x = 1$ mm that corresponds to the deformation $\varepsilon_x = 1$ %. The strain rate was 2 mm.min^{-1}. The boundary conditions are shown in **Figure 5**.

4.1.2. Assembling of extended continuous composite model of long fiber-reinforced composite

The second numerical FEM model, which was created in the concept of structure unit, is formed from three components: fiber matrix—the interfacial interface, where the microscopic dimensions of such a model are closer to the more real composite. Such a model can be created from a structural unit with the $1, 2, \ldots, n$ fibers, wherein the volume geometric configuration (e.g., structural unit is a cube, cuboid, sphere) can affect the volumetric quantity of fibers and a matrix V^f, V^m, as shown by Neckář [12]. The change in volume ratio V^f can be given on the example of the structural unit of the cuboid, which is shown in the section in **Figure 6**. The structural unit consists of six fibers represented by circles with the same spacing m_i, which are

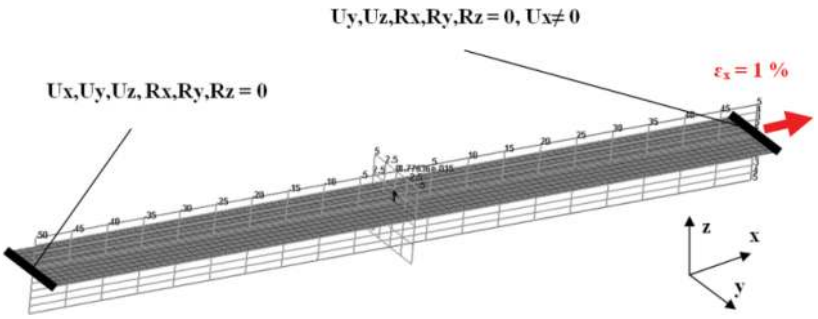

Figure 5. Continuum FEM model of the composite reinforced with long fibers with defined boundary and initial conditions.

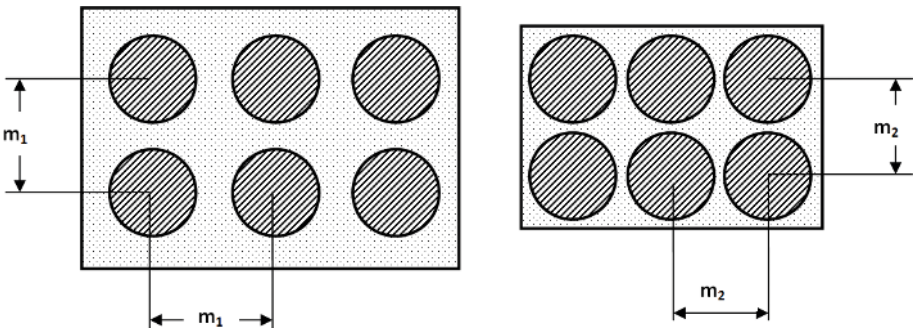

Figure 6. The influence of fiber spacing in the structural unit on V^f fiber volume ratio.

bounded by a matrix (rectangle). By changing of the spacing can then be increased or decreased volume ratio of fibers V^f. The finite element mesh of the numerical model was created from a combination of following elements: BRICK elements (3D elements) with a designed element size of 0.0002 mm defined for fibers and matrix (**Figure 7**).

It will be assumed that $E_{11} = \frac{\sigma_{11}}{\varepsilon_{11}}$, $E_{22} = \frac{\sigma_{22}}{\varepsilon_{22}}$, $G_{12} = \frac{\tau_{12}}{\gamma_{12}}$, $G_{23} = \frac{\tau_{23}}{\gamma_{23}}$.

The problem lies in joining of fibers with the matrix because the interconnections form an interphase. The structural FEM model assembling presents a problem of the determination of appropriate boundary conditions, which is important in terms of accuracy and model verification. Incorrect design may result in concentrators and singularities of stress. The boundary conditions are created by the second type (geometric boundary conditions) as follows: the perimeter surfaces of the model perpendicular to the plane of the stretching direction have defined symmetry conditions on one side (symmetry in axis y and z) and on the opposite side, the boundary conditions are not prescribed. On surfaces in the plane of the stretch direction, that is, in the direction of the X axis, the displacements and rotations were not allowed $U_i = R_i = 0$ in all directions. On the opposite surface of the specimen, the condition was the same, only displacement in the stretching direction was allowed. The displacement was defined constantly to the maximum strain 1%, that is, $U_x = k.|_{\varepsilon_x = 1\%}$, $k. = \text{const.}$, with strain rate 2 mm min^{-1}. Boundary conditions are shown in **Figure 8** and **Table 2**. The material properties applied in both FEM models (I. Continuum Model and the II. Continuum Model with the Structure Unit) are based on the generally known values reported by fiber and matrix manufacturers. The fiber and epoxy matrix parameters are listed in **Table 3**. The results of both numerical simulations have exhibited approximately the same stress at the defined strain $\varepsilon_i = 1\%$ under tensile load in applied direction for a given fiber reinforcement (carbon or glass). The resulting dependence of force on the displacement of the samples obtained from the models showed an approximately linear course, both for carbon and glass fiber-reinforced composite. **Figure 9** shows the tensile test for volume ratio $V^f = 0.3$, where carbon fiber-reinforced composite with the epoxy matrix

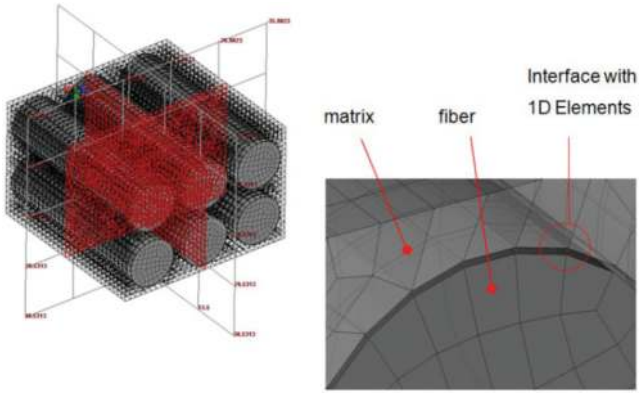

Figure 7. Structural FEM model of a composite reinforced with long fibers.

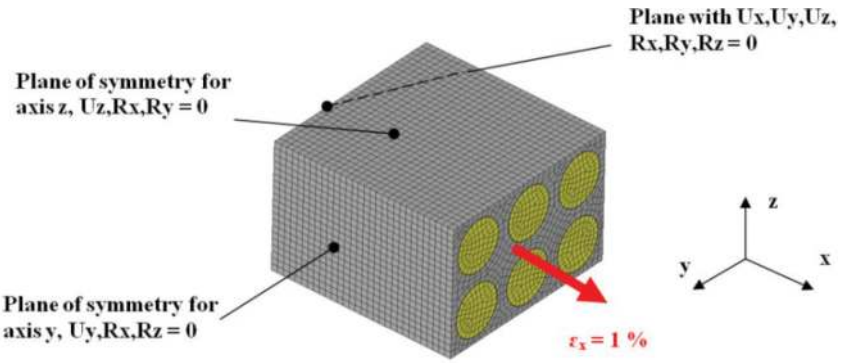

Figure 8. The boundary conditions of the structural FE model of the composite structure reinforced with long fibers.

	Planes in axis x		**Planes in axis y**		**Planes in axis z**	
	$+x$	$-x$	$+y$	$-y$	$+z$	$-z$
E_{11}, μ_{12}	$U_x = k.\|_{\varepsilon_x=1\%}$	$U_i, R_i = 0$	$U_y, R_z, R_x = 0$	—	$U_z, R_x, R_y = 0$	—
E_{22}, μ_{23}	$U_x, R_y, R_z = 0$	—	$U_y = k.\|_{\varepsilon_y=1\%}$	$U_i, R_i = 0$	$U_z, R_x, R_y = 0$	—
G_{12}	$U_y = k.\|_{\varepsilon_y=1\%}$ $U_z = 0$	$U_y = 0$ $U_z = 0$	$U_x = 0$ $U_z = 0$	$U_x = 0$ $U_z = 0$	$U_z = 0$	$U_z = 0$
G_{23}	$U_x = 0$	$U_x = 0$	$U_x = 0$ $U_z = 0$	$U_x = 0$ $U_z = 0$	$U_y = k.\|_{\varepsilon_y=1\%}$ $U_x = 0$	$U_x = 0$ $U_y = 0$

Table 2. FEM model boundary conditions for obtaining elastic constants.

Material	**Density [kg m^{-3}]**	**Modulus of elasticity [GPa]**		**Shear module [GPa]**		**Poisson's ratio [−]**		**Tensile strength [GPa]**	**Elongation [%]**
		$E_{11}^{f,m}$	$E_{22}^{f,m}$	$G_{12}^{f,m}$	$G_{23}^{f,m}$	$\nu_{12}^{f,m}$	$\nu_{23}^{f,m}$		
Carbon fibers	1750 ± 150	230	15	24	5.4	0.279	0.49	2.3 ± 1.2	1.9 ± 0.6
Glass fibers	2370 ± 230	72.4	72.4	28.7	28.7	0.22	0.22	1.06 ± 0.65	4.8 ± 0.7
Epoxy matrix	1150 ± 370	3.573	3.573	1.31	1.31	0.345	0.345	0.067 ± 0.033	3.6

Table 3. Material and mechanical properties of individual constituent of composite.

exhibits approximately 2.2 times higher force response than the glass fiber-reinforced composite with epoxy matrix.

The obtained results shown in **Figures 10** and **11** can be stated that the continuous model (FE model I) has an approximately steady monotonic course manifested not only in continuous

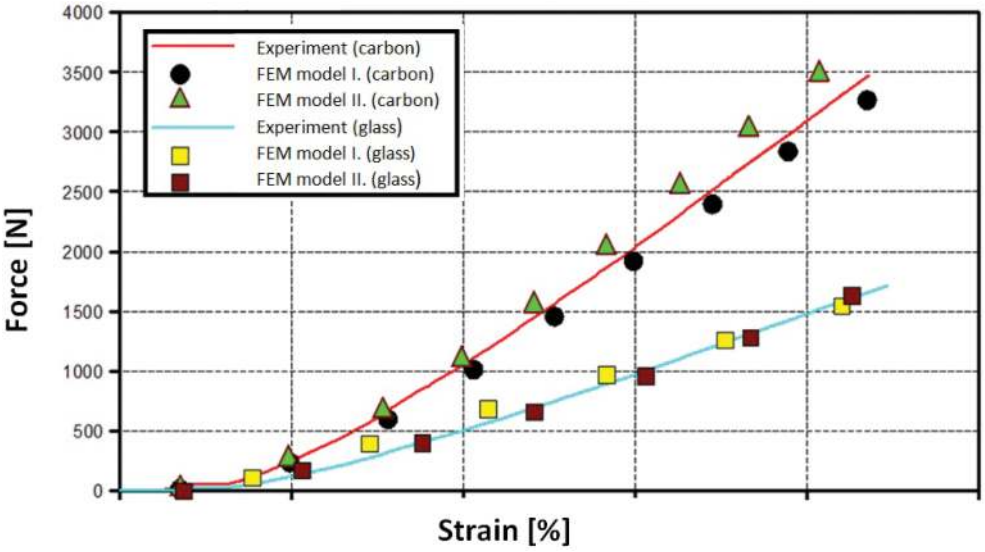

Figure 9. Comparison of experiments and FEM models: Dependence of applied force on sample strain.

distribution of deformation (**Figure 12** above) but also in uniform distribution of the principal stress $\sigma^I = \sigma_{11}$ acting in the load direction (**Figure 12** center).

Due to the simplicity of the FEM model I, it appears to be very suitable for determining the mechanical properties of composite structures and their optimization. However, such a model does not provide information about strain and stress between the fibers and the matrix, let alone the interphase. The continuous model with the structural unit (FEM model II) is significantly more complex, and for some elastic constants, its resultant course is not monotone (G_{23}, ν_{23}); in other words, the resulting dependency is not stable and may not be accurate enough but more complex in terms of results. FEM model II allows to approximate the layout distribution of the structure unit in the loading direction (Z axis) as shown in **Figure 12** (left) and also the principal stress distribution. The principal stress can be determined in isosurfaces or in sequential sections (**Figure 12** right), which allow to analyze the stress distribution between the fibers and the matrix including the interphase. By comparing the maximum values of the stress of 189.1 and 190.9 MPa at same strain $\varepsilon_{11} = 1\%$ and with the volume ratio $V^f = 0.5$ can be stated that the models have significant agreement. This is affected not only by the same material parameters and boundary conditions but also appropriately selected types of elements of the finite element mesh as discussed earlier. FEM model II of the composite structure reinforced with longitudinal fibers with the epoxy matrix is more complex, and the time of the calculation is larger than the FEM model I.

http://dx.doi.org/10.5772/intechopen.71881

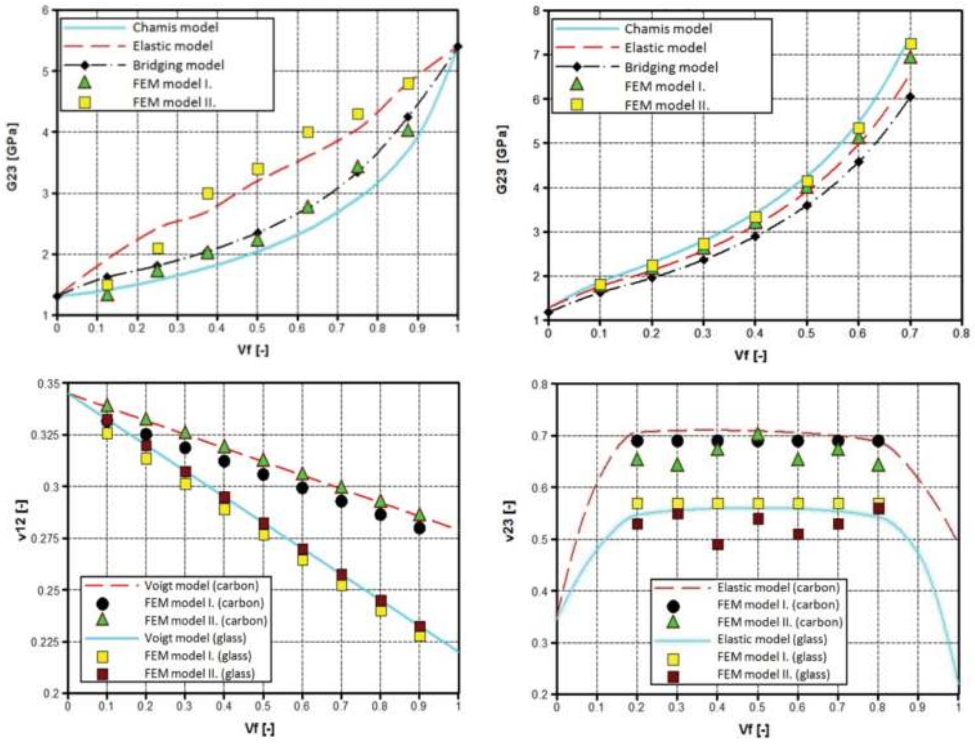

Figure 10. Dependence of modulus G23 (left above), ν_{12} (left below), ν_{23}(right) on V^f of transversally isotropic composites with epoxy matrix and carbon fibers and glass fibers.

However, it must be added that the FEM model II shows valuable scientific knowledge of the approximate distribution of the maximum stress between the fibers and the matrix, which is the largest in the interphase (**Figure 13** left). This confirms the theoretical assumption of the system mechanism (fiber-matrix interphase), where the highest stress transmits newly created component, that is, the interphase, which causes the synergic effect of the resultant construction of the composite structure. **Figure 13** also shows the information that FEM model II shows a nonuniform maximum stress in the composite structure (unlike the FEM model I) and also shows that maximum stress is concentrated only on two fibers (instead of six in the structural unit) of the structural unit. It will reduce the maximum synergic effect that theoretically in the composite structure can occur. The distribution of the interphase in the numerical model and in the real measurement is shown in **Figure 13**. It is necessary to add that from the analyses carried out by measurements on real samples was in all cases evident that the identification of the interphase is very complicated. Due to the

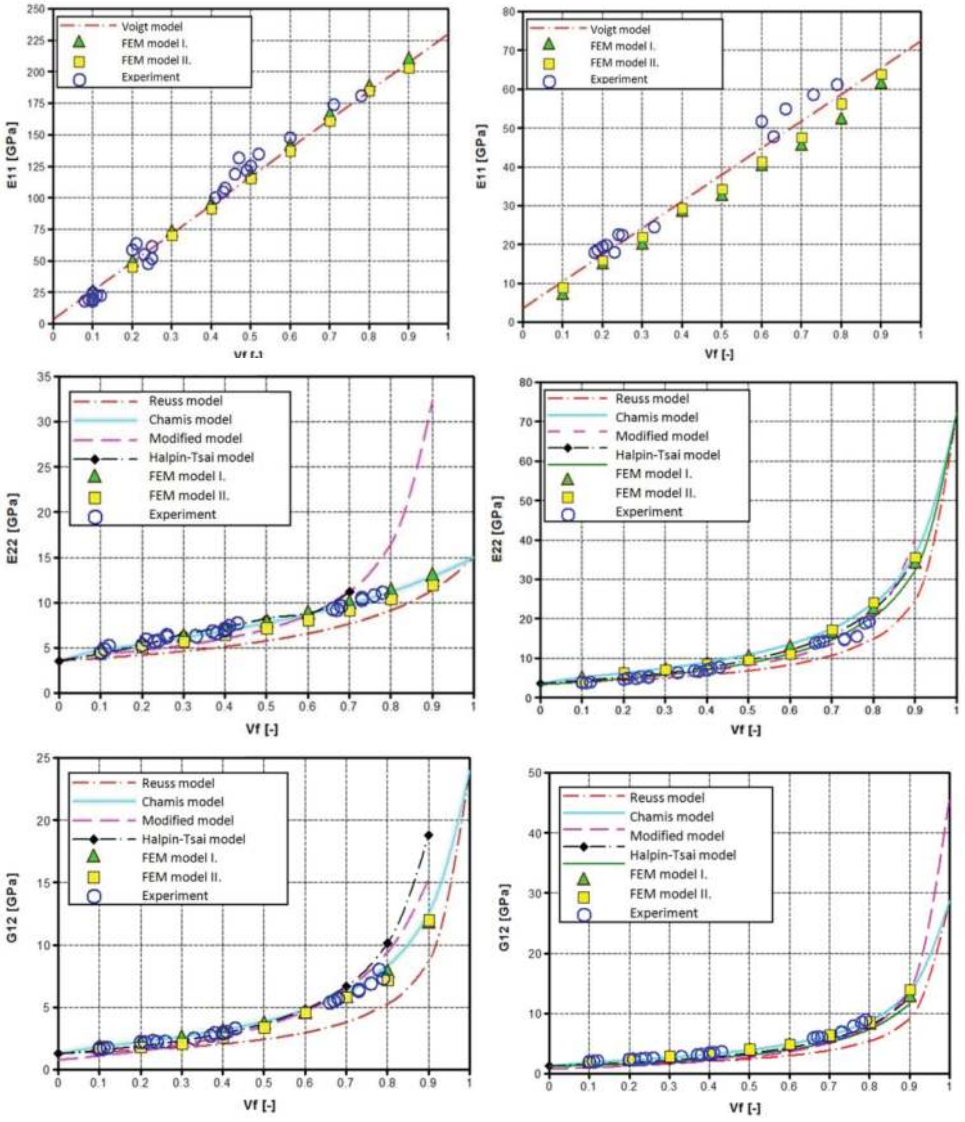

Figure 11. Dependence of modulus *E11, E22, G12* on V^f of transversally isotropic composites with epoxy matrix and carbon fibers (left) and glass fibers (right).

unidentifiable technological process, interphase (third component) could not be created. Also, it is problem to identify and measure the interphase that is important both for verifying of numerical models and for a statistical evaluation how many fibers are involved in synergistic effect.

http://dx.doi.org/10.5772/intechopen.71881

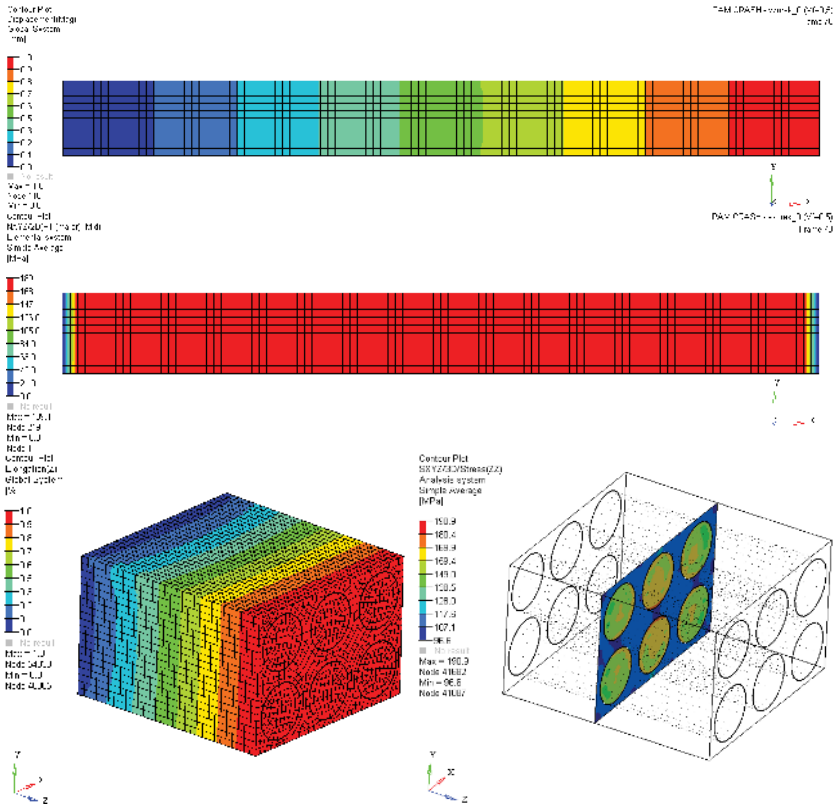

Figure 12. Distribution of deformation (above) and principal stress in the loading direction (center) of the FEM model I of long fiber-reinforced composite with epoxy matrix. The resulting distribution of axial strain (below left) and the principal stress acting in the loading direction (below right) and the FEM model II of composite reinforced with long carbon fiber with epoxy matrix.

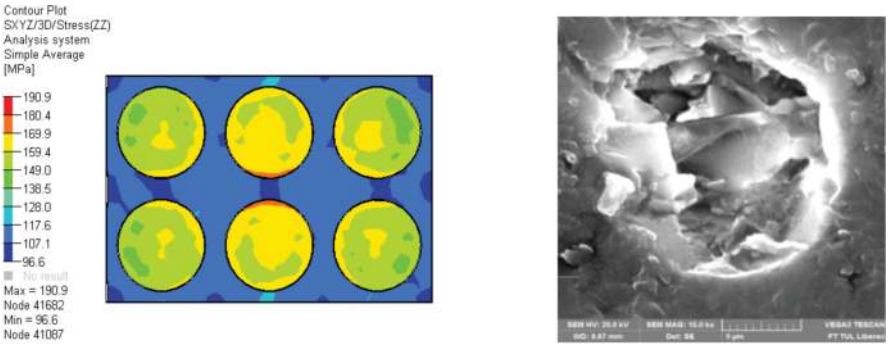

Figure 13. Distribution of principal stress in direction of loading with maximal stress in interphase (left), real sample with visible interphase (right).

5. Conclusion

In this chapter, analyses and numerical simulations of mechanical properties of samples from composite structures were presented. Several studies and experiments have been carried out on samples reinforced with carbon and glass fibers, and mechanical properties allow them to form structural reinforcements of composite materials. Further, analytical models with mathematical relationships (e.g., Voigt, Reuss or Chamis model) allow to determine the unknown elastic constants E_{11}, E_{22}, G_{12}, G_{23}, ν_{12}, ν_{23} of the resulting composite structure. This is followed by a more extensive description of the creation of a numerical model of a composite fiber structure pattern for determining mechanical properties, both through the description of a general continuum and a more complex numerical model with a structural arrangement to allow closer interaction of the fiber and the matrix. From the numerical models, the stress and strain distribution can be determined over a given time interval under chosen packing density V^f as well as the elastic constants. The course of elastic constants has to be compared in some cases only with analytical models because unknown constants cannot be appropriately measured. In summary, the I. continuous model is more user-friendly for numerical simulation and that is suitable for describing the principal stresses, but it does not allow to analyze and study the composite on microlevel. Thus, it does not allow the distribution of the stress between the fiber and the matrix (interphase). This can be done with more complex II. extended continuous model with a structural unit. The results of numerical models establish valuable knowledge and information, including the determination of elastic constants for a particular specific composite design. These results can be used for modeling of large samples and complicated geometries to optimize the design solution.

Author details

Michal Petrů[1]* and Ondřej Novák[2]

*Address all correspondence to: michal.petru@tul.cz

1 Institute for Nanomaterials, Advanced Technology and Innovation, Technical University of Liberec, Liberec, Czech Republic

2 Textile Faculty, Dpt. of Nonwovens and Nanofibrous Material, Technical University of Liberec, Liberec, Czech Republic

References

[1] Agarwal BD, Broutman LJ, Chandrashekhara K. Analysis and Performance of Fiber Composites. 3rd ed. John Wiley & Sons; 2006. p. 576. ISBN: 978-0-471-26891-8

[2] Guedes RM. Creep and Fatigue in Polymer Matrix Composites. Woodhead Publishing; 2011. ISBN: 978-1-84569-656-6

[3] Gay D, Gambelin J. Dimensionnement des Structures, une Introduction. London: Hermes Science Publishing Ltd.; 1999. p. 680. EAN13 : 9782746200494

[4] Reifsnider KL. Fatigue of Composite Materials. Elsevier; 1991. ISBN: 978-0-444-70507-5

[5] Teply JL, Reddy JN. Unified formulation of micromechanics models of fiber-reinforced composites. In: Dvorak GJ, editor. Inelastic Deformation of Composite Materials. New York: Springer; 1990. pp. 341-370

[6] Berthelot JM. Composite Materials: Mechanical Behavior and Structural Analysis. New York: Springer; 1999. pp. 158-181

[7] Gibson RF. Principles of Composite Material Mechanics. New York: Springer: McGraw-Hill, Inc.; 1994. p. 425. ISBN: O-07-023451-5

[8] Soden PD, Hinton MJ, Kaddour AS. Lamina properties, lay-up configurations and loading conditions for a range of fiber-reinforced composite laminates. Composites Science and Technology. 1998;**58**(7):1011-1022. DOI: 10.1016/S0266-3538(98)00078-5

[9] Bareš A. Kompozitní materiály. Praha: SNTL; 1988. p. 356

[10] Gay D, Hoa, SV. Composite Materials – Design and Applications, CRC press, Taylor & Francis Group London, p. 550. ISBN: 978-1-4200-4519-2

[11] Wyk CM. Note on the compressibility of wool. Journal of the Textile Institute. 1946;**37**(12): 285-292

[12] Neckář B, Das D. Modelling of fibre orientation in fibrous materials. Journal of the Textile Institute. 2012;**103**(3):330-340

[13] Petrů M, Novák O, Herák D, Mašín I, Lepšík P, Hrabě P. Finite element method model of the mechanical behaviour of Jatropha Curcas L. bulk seeds under compression loading: Study and 2D modelling of the damage to seeds. Biosystems Engineering. 2014;**127**:50-66. DOI: 10.1016/j.biosystemseng.2014.08.011

[14] Petrů M, Novák O, Herák D, Simanjuntak S. Finite element method model of the mechanical behaviour of Jatropha Curcas L. seed under compression loading. Biosystems Engineering. 2012;**111**:412-421. DOI: 10.1016/j.biosystemseng.2012.01.008

[15] Bittnar Z, Sejnoha J. Numerical Methods in Structural Mechanics, Pitman Monographs and Surveys in Pure and Applied Mathematics. London: Thomas Telford Publications; 1996. p. 442. ISBN: 0-7844-0170-5

[16] Voigt W. Uber die Beziehung zwischen den beiden Elastizitatskonstanten Isotroper Korper. Wiedemanns Annalen der Physik und Chemie (Lepzig). 1889;**38**:573-587

[17] Reuss A. Berechnung der Fliessrense von Mischkristallen auf Grund der Plastizitatsbedingung fur Einkristalle. Zeitschrift Angewandte Mathematik und Mechanik. 1929;**9**:49-58

[18] Younes R, Hallal A, Fardoun F, Chehade FH. Comparative review study on elastic properties modeling for unidirectional composite materials, p. 391-408. Composites and their Properties, INTECH. 2012. DOI: 10.5772/2816

[19] Halpin JC, Kardos JL. The Halpin-Tsai equations: A review. Polymer Engineering and Science. 1976;**16**(5)

[20] Chamis CC. Mechanics of composite materials: Past, present, and future. Journal of Composites, Technology and Research. 1989;**11**(1):3-14. DOI: 10.1520/CTR10143J

[21] Mori T, Tanaka K. Average stress in matrix and average elastic energy of materials with misfitting inclusions. Acta Mettallurgica. 1973;**21**(5):571-574. DOI: 10.1016/0001-6160(73)90064-3

[22] Hill R. Theory of mechanical properties of fibre-strengthen materials – III, self consistent model. Journal of Mechanics and Physics of Solids. 1965;**3**:189-198

[23] Huang ZM. Simulation of the mechanical properties of fibrous composites by the bridging micromechanics model. Composites: Part A. 2001;**32**(3):143-172

[24] Huang ZM, Zhou YX. Strength of unidirectional composites. Advanced Topics in Science and Technology in China. 2012:99-143. DOI: 10.1007/978-3-642-22958-9_4

[25] Li S. Boundary condtions for unit cells from periodic microstructures and their implications. Composites Science and Technology. 2008;**68**(9):1962-1974. DOI: 10.1016/j.compscitech.2007.03.035